Spectroscopic Studies on ZrO_2 Modified with MoO_3 and Activity for Acid Catalysis

Jong Rack Sohn,* Eun Woo Chun, and Young Il Pae†

Department of Industrial Chemistry, Engineering College, Kyungpook National University, Daegu 702-701, Korea
†Department of Chemistry, University of Ulsan, Ulsan 680-749, Korea
Received August 1, 2003

Zirconia modified with MoO_3 was prepared by impregnation of powdered $Zr(OH)_4$ with ammonium heptamolybdate aqueous solution followed by calcining in air at high temperature. Spectroscopic studies on prepared catalysts were performed by using FTIR, Raman, XRD, and DSC and by measuring surface area. Upon the addition of molybdenum oxide to zirconia up to 15 wt%, the specific surface area increased in proportion to the molybdate oxide content, while acidity measured by irreversible chemisorption of ammonia exhibited a maximum value at 3 wt% of MoO_3. Since the ZrO_2 stabilizes the molybdenum oxide species, for the samples equal to or less than 30 wt%, molybdenum oxide was well dispersed on the surface of zirconia and no phase of crystalline MoO_3 was observed at any calcination temperature above 400 °C. The catalytic activities for cumene dealkylation were roughly correlated with the acidity of catalysts measured by ammonia chemisorption method, while the catalytic activities for 2-propanol dehydration were not correlated with the acidity because weak acid sites are necessary for the reaction.

Key Words : MoO_3/ZrO_2 catalyst, Spectroscopic characterization, Acid catalysis, 2-Propanol dehydration, Cumene dealkylation

Introduction

Supported molybdenum oxide catalysts are extremely important for industrial applications. These systems are active for various reactions, such as partial oxidation of hydrocarbons and alcohols,[1-5] hydrogenolysis and hydrodesulfurization of crude oil,[6,7] metathesis of alkenes,[8] hydrogenation of benzene,[9] and cracking of hydrocarbons.[10] The conventional way to prepare the catalysts is to impregnate the high surface area support oxide with an aqueous solution of ammonium heptamolybdate followed by calcining the solid in air. Usually the supports are alumina or silica, but considerable interest is now devoted to other supports such as TiO_2,[11] Nb_2O_5,[12] and ZrO_2.[6,10,13-15] Zirconia is a very interesting material because of its thermal stability, its mechanical properties, and its basic, acidic, reducing, and oxidizing surface properties. Therefore, it is attracting interest in catalysis as a support material as well as a catalyst.

It has been reported by several workers that the addition of platinum to zirconia modified by sulfate ions enhances catalytic activity in the skeletal isomerization of alkanes without deactivation when the reaction is carried out in the presence of hydrogen.[16,17] The high catalytic activity and small deactivation can be explained by both the elimination of the coke by hydrogenation and hydrogenolysis and the formation of Brönsted acid sites from H_2 on the catalysts.[16] Recently, Arata[18] reported zirconia-supported molybdenum oxide as an alternative material in reaction requiring strong acid sites. Several advantages of molybdate, over sulfate, as dopant include that it does not suffer from dopant loss during thermal treatment and it undergoes significantly less deactivation during catalytic reaction. So far, however, supported molybdenum oxide catalysts have been mainly on alumina[19] and silica,[20] and only some work was studied for the ZrO_2 support.[13-15] Moreover, there is no systematic study using a variety of instruments, although some limited work by Raman spectroscopy and X-ray diffraction was reported.[13-15]

This paper describes spectroscopic studies on ZrO_2 modified with MoO_3 and catalytic activity for acid catalysis. The spectroscopic studies of the samples were performed by means of Fourier transform infrared (FTIR), X-ray diffraction (XRD), laser Raman, Differential scanning calorimetry (DSC), and by the measurement of surface area.

Experimental Section

The precipitate of $Zr(OH)_4$ was obtained by adding aqueous ammonia slowly into an aqueous solution of zirconium oxichloride (Aldrich) at room temperature with stirring until the pH of aqueous solution reached about 8.[21-23] The precipitate was washed thoroughly with distilled water until chloride ion was not detected with $AgNO_3$ solution, and was dried at room temperature for 12 h. The dried precipitate was powdered (100 mesh) by grinding.

The catalysts containing various molybdenum oxide contents were prepared by adding an aqueous solution of ammonium heptamolybdate[$(NH_4)_6(Mo_7O_{24})\cdot 4H_2O$] (Aldrich) to the $Zr(OH)_4$ powder followed by drying and calcining at high temperatures for 3 hr in air. This series of catalysts are denoted by their weight percentage of MoO_3 and calcination temperature. For example, 10-MoO_3/ZrO_2(500) indicates the catalyst containing 10 wt% MoO_3 and calcined at 500 °C for 3 hr.

FTIR spectra were obtained in a heatable gas cell at room

*To whom all correspondences should be addressed. Tel: +82-53-950-5585, e-mail: jrsohn@knu.ac.kr

temperature using Mattson Model GL6030E spectrophotometer. The wafers contained about 9 mg/cm^2 self-supporting catalyst. Prior to obtaining the spectra, the samples were heated under vacuum at 400-500 °C for 1.5 hr.

The Raman spectra were obtained with a Spex Ramalog spectrometer with holographic gratings. The 5145-Å line from a Spectra-Physics Model 165 argon-ion laser was used as the exciting source. The laser beam was focussed onto an area 0.1 × 0.1 mm^2 in size of the sample surface; a 90° scattering geometry was used. The spectral shift width was typically 4 cm^{-1}, and laser source powers of approximately 45 mW, measured at the sample, were used.

Catalysts were checked in order to determine the structure of the support as well as that of molybdenum oxide by means of a Jeol Model JDX-8030 diffractometer, employing Ni-filtered Cu K_α radiation.

DSC measurements were performed by a PL-STA model 1500H apparatus in air, and the heating rate was 5 °C per minute. For each experiment 10-15 mg of sample was used.

The acid strength of catalyst was measured qualitatively using a series of the Hammett indicators.[24,25] The catalyst in a glass tube was pretreated at 400 °C for 1 hr and filled with dry nitorgen. For the determination of acid strength of the catalyst the color changes of indicators were observed by spot test. Chemisorption of ammonia was employed as a measure of acidity of catalysts. The amount of chemisorption was obtained as the irreversible adsorption of ammonia.[26,27] Thus the first adsorption of ammonia at 20 °C and 300 torr was followed by evacuation at 230 °C for 1 hr and readsorption at 20 °C, the difference between two adsorptions at 20 °C giving the amount of chemisorption. The specific surface area was determined by applying the BET method to the adsorption of nitrogen at -196 °C.

2-propanol dehydration was carried at 160 and 180 °C in a pulse micro-reactor connected to a gas chromatograph. Fresh catalyst in the reactor made of 1/4 inch stainless steel was pretreated at 400 °C for 1 hr in the nitrogen atmosphere. Diethyleneglycol succinate on Simalite was used as packing material of gas chromatograph and the column temperature was 180 °C for analyzing the product. Catalytic activity for 2-propanol dehydration was represented as mole of propylene converted from 2-propanol per gram of catalyst. Cumene dealkylation was carried out at 400 and 450 °C in the same reactor as above. Packing material for the gas chromatograph was Benton 34 on chromosorb W and column temperature was 130 °C. Catalytic activity for cumene dealkylation was represented as mole of benzene converted from cumene per gram of catalyst. Conversion for both reactions were taken as the average of the first to sixth pulse values.

Results and Discussion

Raman and Infrared Spectra. Raman spectroscopy is a valuable tool for the characterization of dispersed metal oxides and detects vibrational modes of surface and bulk structures. The Raman spectra of MoO_3 obtained by calcining ammonium heptamolybdate at 500 °C, MoO_3/ZrO_2 (500), and ZrO_2 under ambient conditions are presented in Figure 1. The MoO_3 structure is made up of distorted MoO_6 octahedra. Bulk MoO_3 shows the main bands, in good agreement with data previously reported.[28] The major vibrational modes of MoO_3 are located at 995, 819, 667, and 290 cm^{-1}, and have been assigned to the Mo=O stretching mode, the Mo-O-Mo stretching mode, OMo_3 vibration mode, and the Mo=O deformation mode, respectively.[28]

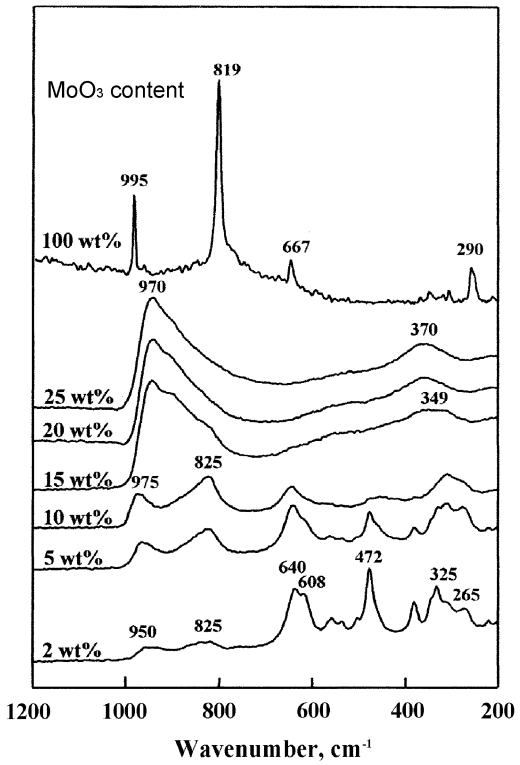

Figure 1. Raman spectra of MoO_3/ZrO_2(500).

The molecular structure of the supported molybdenum oxide species depends on the loading. Several authors observed that the nature of surface molybdenum species on SiO_2, Al_2O_3, TiO_2 and ZrO_2 depends on the amount of MoO_3. A band at about 825 cm^{-1}, corresponding to Mo-O-Mo vibrations,[29,30] and a band at 910-980 cm^{-1}, assigned to M=O vibrations in two dimensional polymolybdate, were observed in these samples.[29,30] Raman bands between 910 and 980 cm^{-1} are usually attributed to the Mo=O vibration of Mo species in either octahedral or tetrahedral environment.[31] Generally, monomolybdate or tetrahedral molybdenum oxygen species have been assigned for low MoO_3 loading samples,[29,31,32] and two-dimensional polymolybdates or octahedral molybdenum-oxygen species with characteristic band around 950-980 cm^{-1}, for high MoO_3 loading samples.[29,31,32] Therefore, the broad band observed in the 900-1000 cm^{-1} region in Figure 1 will be interpreted as an overlap of two characteristic bands for two molybdenum oxide species. The bands around 370 cm^{-1} for 15-MoO_3/ZrO_2, 20-MoO_3/ZrO_2, and 25-MoO_3/ZrO_2 samples are assigned to Mo=O bending mode.[33]

For 15-MoO_3/ZrO_2(500), 20-MoO_3/ZrO_2(500) and 25-

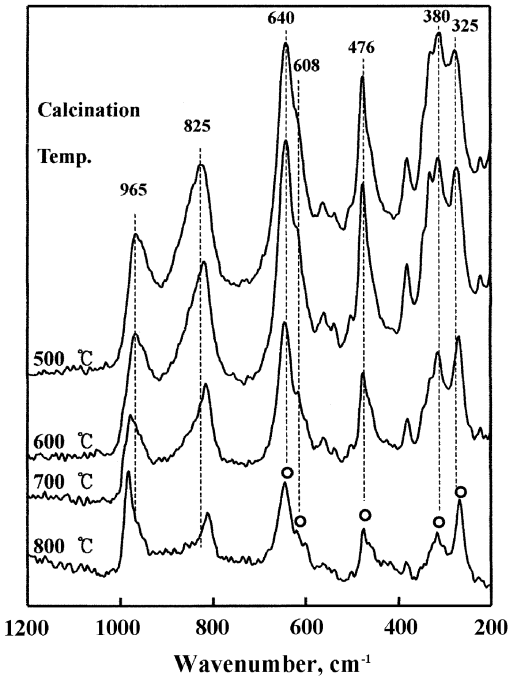

Figure 2. Raman spectra of 5-MoO_3/ZrO_2 calcined at different temperatures: ○, tetragonal phase of ZrO_2.

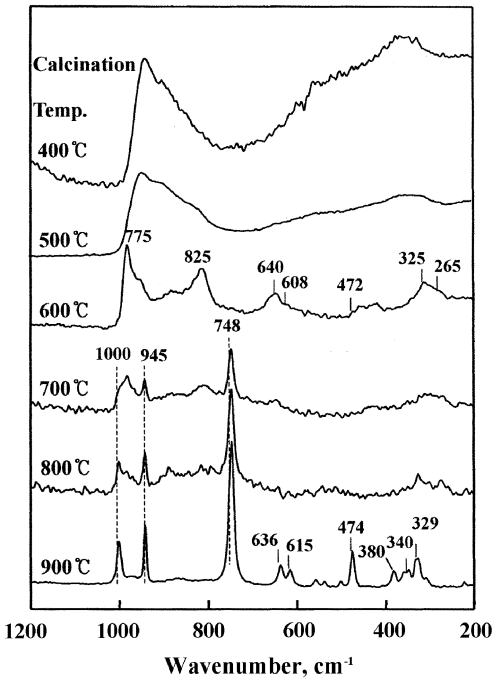

Figure 3. Raman spectra of 15-MoO_3/ZrO_2 calcined at different temperatures.

MoO_3/ZrO_2(500) in Figure 1, most of zirconia is amorphous to X-ray diffraction, showing tiny amount of tetragonal phase zirconia for the other. The Raman spectrum of amorphous zirconia is characterized by a very weak and broad band at 550-600 cm^{-1}.[34] Tetragonal zirconia is expected to yield a spectrum consisting of Raman bands with frequencies at about 148, 263, 325, 472, 608, and 640 cm^{-1}, while monoclinic zirconia exhibits the characteristic features at 180, 188, 221, 380, 476, and 637 cm^{-1}.[35,36] As shown in Figure 1, the 2-MoO_3/ZrO_2, 5-MoO_3/ZrO_2, and 10-MoO_3/ZrO_2 samples exhibit the characteristic features of tetragonal zirconia, indicating no transformation of ZrO_2 from tetragonal to monoclinic.

Figure 2 shows Raman spectra of 5-MoO_3/ZrO_2 samples calcined at 500-800 °C for 3 hr. For all samples, a band around 825 cm^{-1}, corresponding to Mo-O-Mo vibrations,[29,30] and a band around 965 cm^{-1}, assigned to Mo=O vibrations[29,30] in two dimensional polymolybdate, were observed similarly to those of Figure 1. All samples also exhibit the characteristic features of tetragonal zirconia at 265, 325, 472, 608, and 640 cm^{-1}, in good agreement with XRD data described later.

Figure 3 shows Raman spectra of 15-MoO_3/ZrO_2 samples calcined at 400-900 °C for 3 hr. For samples calcined 400-800 °C, a band around 825 cm^{-1} and a band around 965 cm^{-1} were observed similarly to those of Figures 1 and 2. The samples also exhibit the characteristic features of tetragonal zirconia at 500-800 °C. However, the sample calcined at 900 °C exhibit the characteristic features of monoclinic zirconia, indicating the phase transition of ZrO_2 from tetragonal to monoclinic. From calcination temperature of 700 °C, a new species, *i.e.*, $Zr(MoO_4)_2$ phase, identified by its characteristic Raman bands[29] at 748, 944, and 1000 cm^{-1}, has been detected in the 15-MoO_3/ZrO_2 catalyst. As shown in Figure 3, the amount of $Zr(MoO_4)_2$ phase increased with the calcination temperature. Chen *et al.*[15] reported the formation of $Zr(MoO_4)_2$ from MoO_3 and ZrO_2 in high loading sample

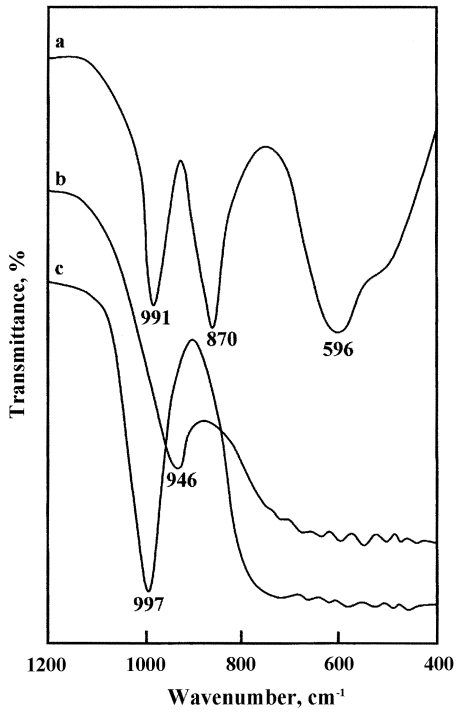

Figure 4. Infrared spectra of (a) bulk MoO_3, (b) 15-MoO_3/ZrO_2(500) evacuated at 25 °C, and (c) 15-MoO_3/ZrO_2(500) evacuated at 500 °C.

calcined above 600 °C.

The Raman spectra in Figures 1-3 have been taken in air using the pure powders. To examine the structure of ZrO_2 modified with MoO_3 under dehydration conditions, IR spectra of 15-MoO_3/ZrO_2 sample were obtained in a heatable gas cell after evacuation at 298 and 773 K for 1.5 h. The IR spectrum for bulk MoO_3 is also presented for the range, 1200-400 cm^{-1} in Figure 4. In view of Raman spectrum of bulk MoO_3 in Figure 1, for bulk MoO_3, the IR bands at 991, 870, and 596 cm^{-1} in Figure 4(a) are assigned to the Mo=O stretching mode, the Mo-O-Mo stretching mode, and OMo_3 vibration mode, respectively. For 15-MoO_3/ZrO_2 sample, IR band at 997 cm^{-1} after evacuation at 773K is due to the Mo=O stretching mode of the molybdenum oxide complex bonded to the ZrO_2 surface.[37] As shown in Figure 4, this Mo=O band due to molybdenyl species only appears on evacuated sample, being shifted on wet sample. The broad band at 946 cm^{-1} under ambient condition [Figure 4(b)] is assigned to the terminal Mo=O stretching of the hydrated form of the surface molybdenyl species.[37] This can be rationalized by assuming that the adsorption of water causes a strong perturbation of the corresponding molybdenum oxide species, with a consequent strong broadening and shift down of this band. This isolated molybdenum oxides species is stabilized through multiple Mo-O-Zr bonds between each molybdenum oxide species and the zirconia surface.[15,29] Upon dehydration at elevated temperature, the hydrated surface metal oxide species is unstable and decompose to form dehydrated surface metal oxide species by direct interaction with the surface OH groups of support, giving the formation of metal-oxygen-support bond.[38]

Crystalline structures of catalysts. The crystalline structures of ZrO_2 and MoO_3/ZrO_2 calcined in air at different temperatures for 3 hr were examined. For pure ZrO_2, ZrO_2 was amorphous to X-ray diffraction up to 300 °C, with a two-phase mixture of the tetragonal and monoclinic forms at 400-700 °C and a monoclinic form at 800 °C (This figure is not shown here). Three crystal structures of ZrO_2, tetragonal, monoclinic and cubic phases have been reported.[39,40]

However, in the case of ZrO_2 modified with MoO_3, the crystalline structures of the samples were different from that of pure ZrO_2. For the 5-MoO_3/ZrO_2, as shown in Figure 5, X-ray diffraction data indicated tetragonal ZrO_2 form at 400-600 °C, and a two-phase mixture of the tetragonal and monoclinic ZrO_2 forms at 700-900 °C. It is assumed that the interaction between molybdenum oxide and ZrO_2 hinders the transition of ZrO_2 from amorphous to tetragonal phase.[21,24] The presence of molybdenum oxide strongly influences the development of textural properties with temperature. No phase of molybdenum oxide was observed at any calcination temperature, indicating a good dispersion of molybdenum oxide on the surface of ZrO_2 support due to the interaction between them. Moreover, for the sample of 15-MoO_3/ZrO_2, the transition temperature from the amorphous to the tetragonal phase was higher by 100 K than that of pure ZrO_2. That is, the more the content of molybdenum oxide, the higher the phase transition temperature. As shown in Figure 7, for 15-MoO_3/ZrO_2, ZrO_2 was amorphous to X-ray diffraction up to 400 °C, with a tetragonal phase of ZrO_2 at 500-700 °C, and a two-phase mixture of the tetragonal and monoclinic ZrO_2 forms at 800-900 °C.

XRD patterns of MoO_3-ZrO_2 containing different MoO_3

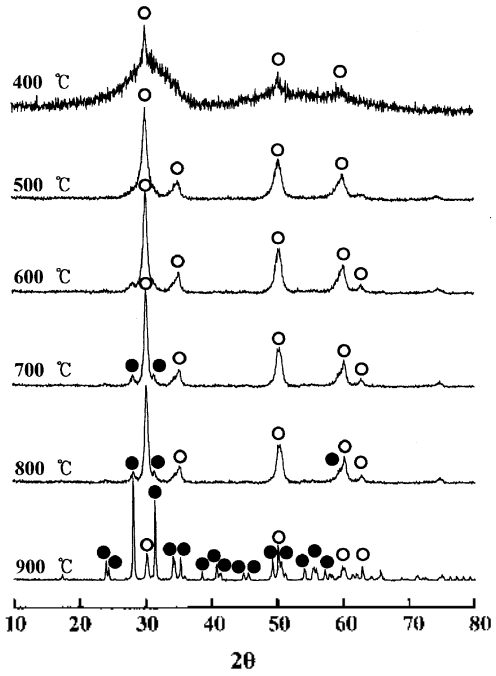

Figure 5. X-ray diffraction patterns of 5-MoO_3/ZrO_2 calcined at different temperatures for 3 hr.: ○, tetragonal phase of ZrO_2; ●, monoclinic phase of ZrO_2.

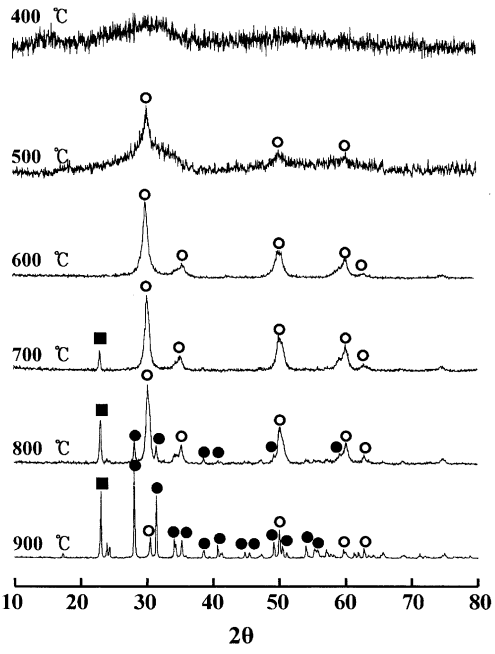

Figure 6. X-ray diffraction patterns of 15-MoO_3/ZrO_2 calcined at different temperatures for 3 hr.: ○, tetragonal phase of ZrO_2; ●, monoclinic phase of ZrO_2; ■, $Zr(MoO_4)_2$ phase.

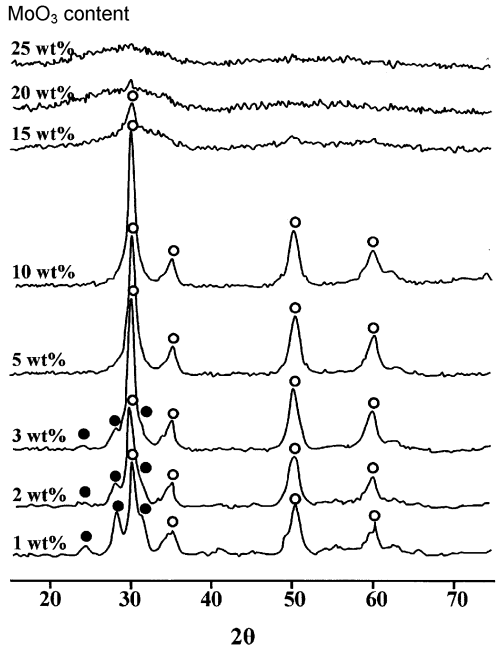

Figure 7. X-ray diffraction patterns of MoO_3-ZrO_2 containing different MoO_3 contents and calcined at 500 °C for 3 hr.: ○, tetragonal phase of ZrO_2; ●, monoclinic phase of ZrO_2.

contents and calcined at 500 °C for 3 hr are shown in Figure 7. ZrO_2 is a two-phase mixture of the tetragonal and monoclinic forms up to 3 wt%, but for sample containing MoO_3 equal to or above 15 wt%, ZrO_2 was amorphous because the interaction between MoO_3 and ZrO_2 hinders the phase transition of ZrO_2 from amorphous to tetragonal phase.[21,24]

It is also of interest to examine the influence of molybdenum oxide on the transition temperature of ZrO_2 from tetragonal to monoclinic phase. In view of X-ray diffraction patterns, the calcination temperatures at which monoclinic phase is observed initially are 500 °C for pure ZrO_2, 700 °C for 5-MoO_3/ZrO_2, 800 °C for 15-MoO_3/ZrO_2, respectively. That is, the transition temperature increases with increasing molybdenum oxide content. This can be also explained in terms of the delay of transition from tetragonal to monoclinic phase due to the interaction between molybdenum oxide and zirconia, in analogy with the delay of transition from amorphous to tetragonal phase described above. For 15-MoO_3/ZrO_2, the XRD patterns clearly show the formation of $Zr(MoO_4)_2$ from MoO_3 and ZrO_2 at 700-900 °C, showing the increased amount of $Zr(MoO_4)_2$ phase with the calcination temperature. These results are in good agreement with those of Raman spectra in Figure 3.

Thermal Analysis. In X-ray diffraction pattern, it was shown that the structure of MoO_3/TiO_2 was different depending on the calcined temperature. To examine the thermal properties for the precusors of samples more clearly, their thermal analysis was carried out and illustrated in Figure 8. For pure ZrO_2 the DSC curve showed a broad endothermic peak below 180 °C due to the elimination of adsorbed water, and an exothermic peak at 430 °C due to the

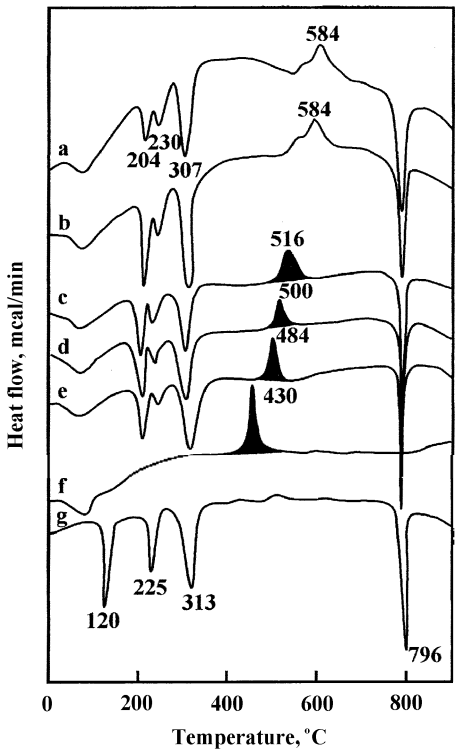

Figure 8. DSC curves of precursors of catalysts: (a) 25-MoO_3/ZrO_2, (b) 15-MoO_3/ZrO_2, (c) 10-MoO_3/ZrO_2, (d) 5-MoO_3/ZrO_2, (e) 1-MoO_3/ZrO_2, (f) ZrO_2, and (g) $(NH_4)_6(Mo_7O_{24})\cdot 4H_2O$.

ZrO_2 crystallization.[21,35] In the case of MoO_3/ZrO_2, three additional endothermic peaks appeared in the region of 200-400 °C due to the evolution of NH_3 and H_2O decomposed from ammonium heptamolybdate. Also it is considered that an endothermic at 796 °C is responsible for melting of MoO_3 and an exothermic peaks around 584 °C is due to the formation of $Zr(MoO_4)_2$ described in X-ray diffraction patterns. However, it is of interest to see the influence of MoO_3 on the crystallization of ZrO_2 from amorphous to tetragonal phase. As Figure 8 shows, the exothemic peak due to the crystallization appears at 430 °C for pure ZrO_2, while for MoO_3/ZrO_2, it was shifted to higher temperatures. The shift increased with increasing MoO_3 content up to 10 wt% of MoO_3. It is considered that the interaction between MoO_3

Table 1. Specific surface area and acidity of MoO_3/ZrO_2 catalysts calcined at 500 °C for 3 hr

Catalyst	Surface area (m^2/g)	Acidity (μmol/g)
ZrO_2	58	45
1-MoO_3/ZrO_2	111	159.3
2-MoO_3/ZrO_2	113	161.5
3-MoO_3/ZrO_2	121	167.1
5-MoO_3/ZrO_2	135	137.9
10-MoO_3/ZrO_2	171	127.6
15-MoO_3/ZrO_2	193	120.11
20-MoO_3/ZrO_2	188	113.7
25-MoO_3/ZrO_2	151	95.3
30-MoO_3/ZrO_2	105	89.9

Table 2. Acid Strengths of Some Samples

Hammett indicator	pKa	ZrO_2	5-MoO_3/ZrO_2(500)
Benzeneazodiphenylamine	+1.5	+	+
Dicinnamalacetone	−3.0	−	+
Benzalacetophenone	−5.6	−	+
Anthraquinone	−8.2	−	+
Nitrobenzene	−12.4	−	+
2,4-dinitrofluorobenzene	−14.5	−	+

and ZrO_2 delays the transition of ZrO_2 from amorphous to anatase phase.[26] Consequently, the exothermic peaks appear at 484 °C for 1-MoO_3/ZrO_2, 500 °C for 5-MoO_3/ZrO_2, and 516 °C for 10-MoO_3/ZrO_2. These results are in good agreement with those of XRD described above.

Surface Properties. It is necessary to examine the effect of molybdenum oxide on the surface properties of catalysts, that is, specific surface area, acidity, and acid strength. The specific surface areas of samples calcined at 500 °C for 3 hr are listed in Table 1. The presence of molybdenum oxide strongly influences the surface area in comparison with the pure ZrO_2. Specific surface areas of MoO_3/ZrO_2 samples are much larger than that of pure ZrO_2 calcined at the same temperature, showing that surface area increases gradually with increasing molybdenum oxide content up to 15 wt% of MoO_3. It seems likely that the interaction between molybdenum oxide and ZrO_2 protects catalysts from sintering.

The acid strength of the catalysts was examined by a color change method, using Hammett indicator in sulphuryl chloride.[21,27] The results are listed in Table 2. In this table, (−) indicates that the color of the base form was changed to that of the conjugated acid form. ZrO_2 evacuated at 400 °C for 1 h has an acid strength $H_0 \leq +1.5$, while 5-MoO_3/ZrO_2 was estimated to have a $H_0 \leq -14.5$, indicating the formation of new acid sites stronger than those of single oxide components. Acids stronger than $H_0 \leq -11.93$, which corresponds to the acid strength of 100% H_2SO_4, are superacids.[22] Consequently, MoO_3/ZrO_2 catalysts would be solid superacids. The superacidic property is attributed to the double bond nature of the Mo=O in the complex formed by the interaction of ZrO_2 with molybdate, in analogy with the case of ZrO_2 modified with tungstate, chromate, and sulfate ion.[21,22,25,27]

The acidity of catalysts calcined at 500 °C, as determined by the amount of NH_3 irreversibly adsorbed at 230 °C,[21,24] is listed in Table 1. As listed in Table 1, the acidity increases upon the addition of 1 wt% molybdenum oxide to ZrO_2, giving a maximum at 3 wt% of MoO_3, and then the acidity decreases with increasing molybdenum oxide content. Many combinations of two oxides have been reported to generate acid sites on the surface.[41] The combination of ZrO_2 and MoO_3 probably generates stronger acid sites and more acidity as compared with the separate components. However, the surface area exhibited a maximum at 15 wt% of MoO_3, as listed in Table 1. That is, the maximum values in surface area and acidity appears at different MoO_3 content,

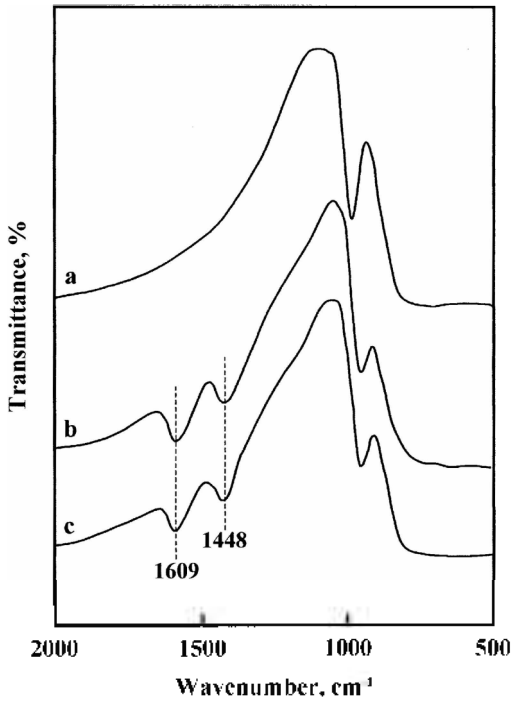

Figure 9. Infrared spectra of NH_3 adsorbed on 5-MoO_3/ZrO_2(500): (a) background of 5-MoO_3/ZrO_2(500) evacuated at 400 °C, (b) NH_3 adsorbed on 5-MoO_3/ZrO_2(500), and (c) b sample evacuated at 230 °C for 0.5 hr.

respectively. Such differences are probably due to the basicity of ammonia or due to the different extent which ammonia and N_2 diffuse into the interior of MoO_3/ZrO_2 micro-pores, respectively. In fact, it is known that the various bases are adsorbed to different extents even by the same catalyst.[41]

Infrared spectroscopic studies of ammonia adsorbed on

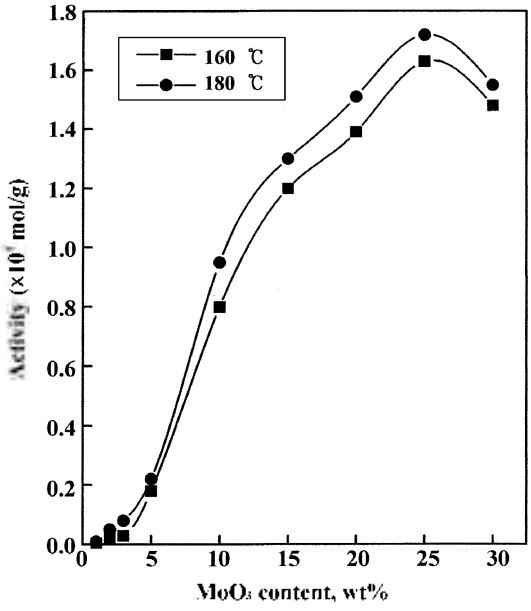

Figure 10. Catalytic activities of MoO_3/ZrO_2(500) for 2-propanol dehydration as a function of MoO_3 content.

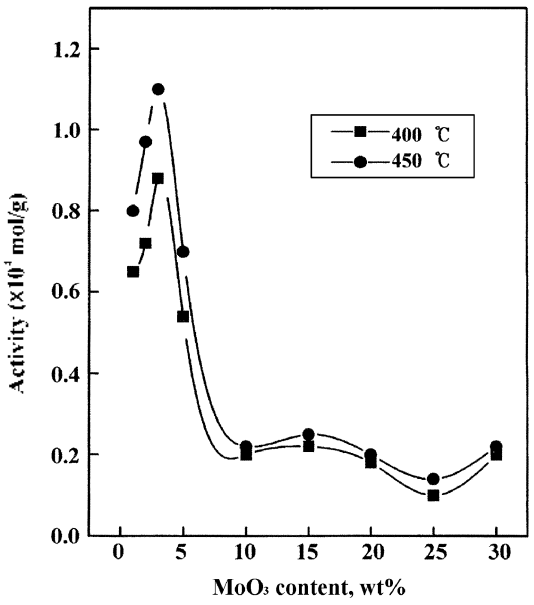

Figure 11. Catalytic activities of $MoO_3/ZrO_2(500)$ for cumene dealkylation as a function of MoO_3 content.

solid surface have made it possible to distinguish between Brönsted and Lewis acid sites.[42] Figure 9 shows the IR spectra of ammonia adsorbed on 5-$MoO_3/ZrO_2(500)$ evacuated at 400 °C for 1 hr. For 5-$MoO_3/ZrO_2(500)$, the bands at 1448 are the characteristic peaks of ammonium ion, which are formed on the Brönsted acid sites and the other set of adsorption peaks at 1609 cm^{-1} is contributed by ammonia coordinately bonded to Lewis acid sites,[42] indicating the presence of both Brönsted and Lewis acid sites. Other samples having different MoO_3 contents also showed the presence of both Lewis and Brönsted acid sites. Therefore, these MoO_3/ZrO_2 samples can be used as catalysts for Lewis or Brönsted acid catalysis.

Catalytic activities for acid catalysis. It is interesting to examine how the catalytic activity of acid catalyst depends on the acidic property. The catalytic activities for the 2-propanol dehydration and cumene dealkylation are measured and the results are illustrated as a function of MoO_3 content in Figures 10 and 11, respectively, where reaction temperatures are 160-180 °C for 2-propanol dehydration and 400-450 °C for cumene dealkylation. In view of Table 2 and Figures 10 and 11, the variation in catalytic activity for 2-propanol dehydration is not correlated with the change of acidity. However, the variation in catalytic activity for cumene dealkylation is roughly correlated with that of acidity. The differences of catalytic activities for both reactions against acidity are due to the difference of necessary acid strength for both reactions to occur. In fact, it has been known that 2-propanol dehydration takes place very readily on weak acid sites, while cumene dealkylation does on relatively strong acid sites.[43] Therefore, in the case of $MoO_3/ZrO_2(500)$, it is concluded that the number of weak acid sites is maximum for 25-$MoO_3/ZrO_2(500)$, while that of strong acid sites is maximum for 3-$MoO_3/ZrO_2(500)$. In view of the catalytic data shown in Figures 10 and 11 for 2-propanol dehydration and cumene dealkylation reactions, where the reaction temperature were 160-180 °C for the former and 400-450 °C for the latter, it is clear that 2-propanol dehydration takes place more readily than cumene dealkylation.

Conclusions

This paper has shown that a combination of FTIR, Raman spectroscopy, DSC, and XRD can be used to perform the characterization of MoO_3/ZrO_2 prepared by modifying ZrO_2 with MoO_3 and calcining in air. The interaction between molybdunum oxide and zirconia influences the physicochemical properties of prepared catalysts with calcination temperature. The specific surface area of $MoO_3/ZrO_2(500)$ increased in proportion to the molybdenum oxide content up to 15 wt%. Since the ZrO_2 stabilizes the surface molybdenum oxide species, for the samples equal to or less than 30 wt%, molybdenum oxide was well dispersed on the surface of zirconia, showing no phase of crystalline MoO_3 at any calcination temperature. Upon the addition of only a small amount of molybdenum oxide (1 wt%) to zirconia, both the acidity and acid strength of the catalyst increases remarkably, showing the presence of Brönsted and Lewis acid sites on the surface of MoO_3/ZrO_2. The high acid strength and high acidity are responsible for the Mo=O bond nature of complex formed by the interaction between MoO_3 and ZrO_2. The catalytic activities of MoO_3/ZrO_2 catalysts for cmene dealkylation were roughly correlated with their acidity, while those for 2-propanol dehydration which takes place readily on weak acid sites were not correlated with the acidity.

Acknowledgements. This research was supported by Kyungpook National University Research Team Fund, 2002 and was partially supported by grant No. (R05-2003-000-10074-0) from the Basic Research Program of the Korea Science and Engineering Foundation. We wish to thank Korea Basic Science Institute (Daegu Branch) for the use of X-ray diffractometer and Raman spectrometer.

References

1. Martin, C.; Martin, I.; Rives, V. *J. Chem. Soc. Faraday Trans.* **1993**, *89*, 4131.
2. Niwa, M.; Yamada, H.; Murakami, Y. *J. Catal.* **1992**, *134*, 331.
3. Matsuoka, Y.; Niwa, M.; Murakami, Y. *J. Phys. Chem.* **1990**, *94*, 1477.
4. Miyata, H.; Tokuda, S.; Ono, T.; Ohno, T.; Hatayama, F. *J. Chem. Soc., Faraday Trans.* **1990**, *86*, 2291.
5. Miyata, H.; Tokuda, S.; Ono, T.; Ohno, T.; Hatayama, F. *J. Chem. Soc., Faraday Trans.* **1990**, *86*, 3659.
6. Afanasiev, P.; Geantet, C.; Breysse, M. *J. Catal.* **1995**, *153*, 17.
7. Okamoto, Y.; Imanaka, T.; Teramishi, S. *J. Phys. Chem.* **1981**, *85*, 3798.
8. Ono, T.; Anpo, M.; Kabokawa, Y. *J. Phys. Chem.* **1986**, *90*, 4780.
9. Quincy, R. B.; Houalla, M.; Proctor, A.; Hercules, D. M. *J. Phys. Chem.* **1990**, *94*, 1520.
10. Zhao, B.; Wang, X.; Ma, H.; Tang, Y. *J. Mol. Catal. A: Chemical* **1996**, *108*, 167.
11. Ng, K. Y. S.; Guilari, E. *J. Catal.* **1985**, *92*, 340.

12. Jin, Y. S.; Auroux, A.; Védrine, J. C. *J. Chem. Soc. Faraday Trnas.* **1989**, *83*, 4179.
13. Maity, S. K.; Rana, M. S.; Srinivas, B. N.; Bej, S. K.; Murali, Dhar, G.; Prasada Rao, T. S. R. *J. Mol. Catal. A: Chemical* **2000**, *153*, 121.
14. Brown, A. S. C.; Hargreaves, J. S. J.; Taylor, S. H. *Catal. Lett.* **1999**, *57*, 109.
15. Chen, K.; Xie, S.; Tglesia, E.; Bell, A. T. *J. Catal.* **2000**, *189*, 421.
16. Ebitani, K.; Konish, J.; Hattori, H. *J. Catal.* **1991**, *130*, 257.
17. Vaudagna, S. R.; Conelli, R. A.; Canavese, S. A.; Figoli, N. S. *J. Catal.* **1997**, *169*, 389.
18. Arata, K. *Adv. Catal.* **1990**, *37*, 165.
19. Imamura, S.; Sasaki, H.; Shono, M.; Kanai, H. *J. Catal.* **1998**, *177*, 72.
20. Desikan, A. N.; Huang, L.; Oyama, S. T. *J. Phys. Chem.* **1991**, *95*, 10050.
21. Sohn, J. R. *J. Ind. Eng. Chem.* **2004**, *10*, in press.
22. Sohn, J. R.; Kwon, T. D.; Kim, S. B. *J. Ind. Eng. Chem.* **2001**, *7*, 441.
23. Sohn, J. R.; Seo, K. C.; Pae, Y. I. *Bull. Korean Chem. Soc.* **2003**, *24*, 311.
24. Sohn, J. R.; Cho, S. G.; Pae, Y. I.; Hayashi, S. *J. Catal.* **1996**, *159*, 170.
25. Sohn, J. R.; Park, M. Y. *Langmuir* **1998**, *14*, 6140.
26. Sohn, J. R.; Ozaki, A. *J. Catal.* **1980**, *61*, 29.
27. Sohn, J. R.; Ryu, S. G. *Langmuir* **1993**, *9*, 126.
28. Smith, M. R.; Ozkan, U. S. *J. Catal.* **1993**, *141*, 124.
29. Liu, Z.; Chen, Y. *J. Catal.* **1998**, *177*, 314.
30. Mestl, G.; Srinivasan, T. K. K. *Cat. Rev. Sci. Eng.* **1998**, *40*, 451.
31. Dufresne, P.; Payen, E.; Grimblot, J.; Bonnelle, J. P. *J. Phys. Chem.* **1981**, *85*, 2344.
32. Hu, H.; Wachs, I. E. *J. Phys. Chem.* **1995**, *99*, 10897.
33. Roark, R. D.; Kohler, S. D.; Ekerdt, J. G.; Kim, D. S.; Wachs, I. E. *Catal. Lett.* **1992**, *16*, 77.
34. Schild, C. H.; Wokaun, A.; Köppel, R. A.; Baiker, A. *J. Catal.* **1991**, *130*, 657.
35. Sohn, J. R.; Doh, I. J.; Pae, Y. I. *Langmuir* **2002**, *18*, 6280.
36. Scheithauer, M.; Grasselli, R. K.; Knözinger, H. *Langmuir* **1998**, *14*, 3019.
37. Litteti, L.; Nova, I.; Ramis, G.; DallAcqua, L.; Busca, G.; Giamello, E.; Forzatti, P.; Bregani, F. *J. Catal.* **1999**, *187*, 419.
38. Kim, D. S.; Ostromecki, M.; Wachs, I. E. *J. Mol. Catal. A: Chemical* **1996**, *106*, 93.
39. Larsen, G.; Lotero, E.; Petkovic, L. M.; Shobe, D. S. *J. Catal.* **1997**, *169*, 67.
40. Afanasiev, P.; Geantet, C.; Breysse, M.; Coudurier, G.; Vedrine, J. C. *J. Chem. Soc., Faraday Trans., 1* **1994**, *190*, 193.
41. Tanabe, K.; Misono, M.; Ono, Y.; Hattori, J. *New Solid Acids and Bases*; Elsevier Science: Amsterdam, 1989; p 108.
42. Satsuma, A.; Hattori, A.; Mizutani, K.; Furuta, A.; Niyamoto, A.; Hattori, T.; Murakami, Y. *J. Phys. Chem.* **1988**, *92*, 6052.
43. DeCanio, S. J.; Sohn, J. R.; Fritz, P. O.; Lunsford, J. H. *J. Catal.* **1986**, *101*, 132.